Reflection and transmission of Gaussian beam by a chiral slab

[1]Bing Yan, [2,*]Chenhua Liu, [3]Huayong Zhang, and [4]Jianyong Zhang

[1]School of Information and Communication Engineering. North University of China, Taiyuan, Shanxi 030051, China
[2]Department of Mathematics, Application Science Institute, Taiyuan University of Science and Technology, Taiyuan, Shanxi 030024, China
[3]School of Electronics and Information Engineering, Anhui University, Hefei, Anhui 230039, China
[4]School of Science and Engineering, Teesside University, Middlesbrough, UK

Based on the generalized Lorenz-Mie theory framework, the reflection and transmission of an incident Gaussian beam by a chiral slab were investigated, by expanding the incident Gaussian beam, reflected beam, internal beam as well as transmitted beam in terms of cylindrical vector wave functions. The unknown expansion coefficients were determined by virtue of the boundary conditions. For a localized beam model, numerical results of the normalized field intensity distributions are presented, and the propagation characteristics are discussed concisely in this paper.

1. INTRODUCTION

The interaction of electromagnetic (EM) waves with chiral media has drawn considerable attention over the years, for many potential applications involving antennas, antenna radomes (chiral covers), microstrip substrates, and waveguides. Owing to the optical activity, in a chiral medium a linearly polarized wave undergoes a rotation of its polarization as it propagates, and there exist two eigenwaves, the right and left circularly polarized waves (RCP and LCP waves) with different phase velocities. For many fundamental canonical problems, analytical solutions have been provided. The EM plane wave scattering by an optically active sphere or cylinder has been analyzed by using the vector wave functions [1, 2]. On implementation of the EM boundary conditions for the corresponding characteristic plane waves, a theoretical study has been presented of the plane wave propagation through a dielectric-chiral interface and through a chiral slab [3, 4]. As for the case of a shaped beam, which is of practical importance, Yokota et al. studied the scattering of a Hermite-Gaussian beam by a chiral sphere via establishing the relations between the multipole fields and the conventional Hermite-Gaussian beam [5]. By using an angular spectrum of plane waves to represent the incident field, the refraction at a dielectric-chiral interface of near fields of a constant current line source has been examined by Lakhtakia et al. [6], and of a two-dimensional (2D) Gaussian beam by Hoppe et al. [7]. Adopting the same angular spectrum representation approach, Huang et al. discussed the lateral shifts from a slab of lossy chiral metamaterial illuminated by a 2D Gaussian beam [8]. The light pressure exerted on a chiral sphere by a Gaussian beam has also recently been studied [9]. In one recent paper [10], within the generalized Lorenz-Mie theory (GLMT) framework we have obtained an explicit description of the expansion of a Gaussian beam (focused TEM_{00} mode laser beam) in terms of cylindrical vector wave functions (CVWFs). In this paper, the use of such an expansion enables us to construct an analytical solution to the reflection and transmission of a Gaussian beam by a chiral slab.

The body of this paper proceeds as follows. Section 2 provides a theoretical procedure for the determination of the reflected, internal and transmitted fields for a Gaussian beam incident on a chiral slab. In Section 3, numerical results of the normalized field intensity distributions are presented, and the conclusions are drawn in Section 4.

2. FORMULATION

2.1 Expansions of Gaussian beam, reflected beam and transmitted beam in cylindrical coordinates

As shown in Fig.1, the planes $z=0$ and $z=d$ of the Cartesian coordinate system $Oxyz$ are the interfaces between the free space and a chiral slab of thickness d with an infinite area. An incident Gaussian beam propagates along the axis $O'z'$ which lies in the plane xOz of the system $Oxyz$, with the middle of its beam waist located at origin O' on the axis $O'z'$. The angle of incidence or the angle made by the axis $O'z'$ with the axis Oz is β, and origin O of the system $Oxyz$ has a coordinate z_0 on the axis $O'z'$. In this paper, the time-dependent part of the EM fields is assumed to be $\exp(-i\omega t)$.

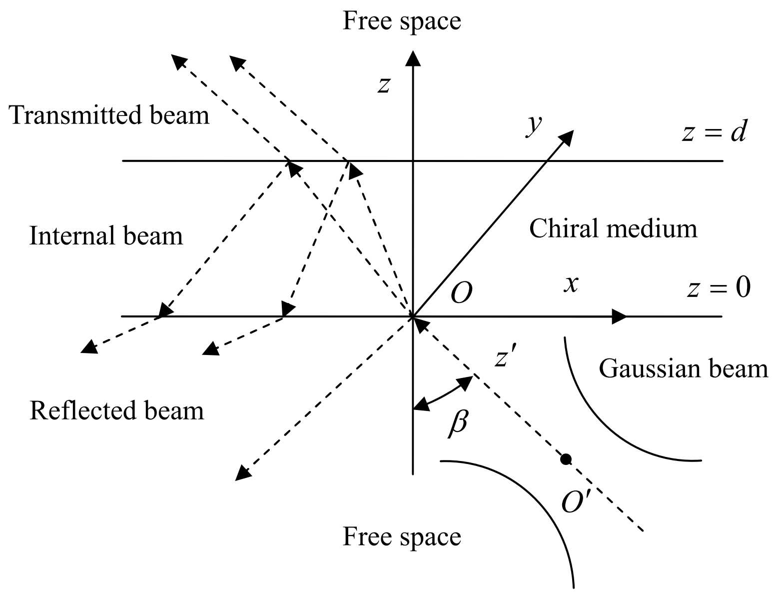

Fig.1. Geometry of an incident Gaussian beam from free space on a chiral slab

In [10], by transforming the spherical vector wave functions into the CVWFs [11], an EM field expansion of an incident Gaussian beam (focused TEM_{00} mode laser beam) has been obtained in terms of the CVWFs in the system $Oxyz$, which, for the sake of subsequent applications of boundary conditions, can be written as

$$\mathbf{E}^i = \mathbf{E}_1^i + \mathbf{E}_2^i \tag{1}$$

where the electric field $\mathbf{E}_1^i$ is described as [10, 12]

$$\mathbf{E}_1^i = E_0 \sum_{m=-\infty}^{\infty} \int_0^{\frac{\pi}{2}} [I_{m,TE}(\zeta)\mathbf{m}_{m\lambda}^{(1)}(h) + I_{m,TM}(\zeta)\mathbf{n}_{m\lambda}^{(1)}(h)]\exp(ihz)d\zeta \tag{2}$$

and $\mathbf{E}_2^i$ is the same expression as $\mathbf{E}_1^i$, except that the integrated range of ζ is from $\pi/2$ to π.

In Eq. (2), $\lambda = k_0 \sin\zeta$, $h = k_0 \cos\zeta$, k_0 is the free-space wavenumber, and $I_{m,TE}$, $I_{m,TM}$ are the Gaussian beam shape coefficients.

For a TE polarized Gaussian beam, the coefficients $I_{m,TE}$, $I_{m,TM}$ are

$$I_{m,TE} = \frac{(-i)^{m+1}}{k_0} \sum_{n=|m|}^{\infty} \frac{(n-m)!}{(n+m)!} \frac{2n+1}{2n(n+1)} g_n [m^2 \frac{P_n^m(\cos\beta)}{\sin\beta} \frac{P_n^m(\cos\zeta)}{\sin\zeta} + \frac{dP_n^m(\cos\beta)}{d\beta} \frac{dP_n^m(\cos\zeta)}{d\zeta}] \tag{3}$$

$$I_{m,TM} = \frac{(-i)^{m+1}}{k_0} m \sum_{n=|m|}^{\infty} \frac{(n-m)!}{(n+m)!} \frac{2n+1}{2n(n+1)} g_n [\frac{P_n^m(\cos\beta)}{\sin\beta} \frac{dP_n^m(\cos\zeta)}{d\zeta} + \frac{dP_n^m(\cos\beta)}{d\beta} \frac{P_n^m(\cos\zeta)}{\sin\zeta}] \tag{4}$$

where g_n (Gaussian beam shape coefficients in spherical coordinates), when the Davis-Barton model of the Gaussian beam is used [13], can be computed with its localized approximation as [14, 15]

$$g_n = \frac{1}{1+2isz_0/w_0}\exp(ikz_0)\exp\left[\frac{-s^2(n+1/2)^2}{1+2isz_0/w_0}\right] \tag{5}$$

where $s = 1/(k_0 w_0)$, and w_0 is the beam waist radius.

For a TM polarized Gaussian beam, its corresponding expansions can be obtained by replacing the coefficients $I_{m,TE}$ with $iI_{m,TM}$, and $I_{m,TM}$ with $iI_{m,TE}$.

It is worth mentioning that the coefficients $I_{m,TE}$, $I_{m,TM}$ in Eqs. (3) and (4) are expressed in terms of beam shape coefficients in spherical coordinates. Obviously it is an extrinsic method. Gouesbet et al. introduced an intrinsic method known as "cylindrical localized approximation" to evaluate the coefficients [16].

Equation (1) can be interpreted as an incident Gaussian beam being expanded into a continuous spectrum of cylindrical vector waves, with each cylindrical vector wave having a propagation vector $\mathbf{k}_0 = \lambda\hat{r} + h\hat{z}$. The angle between $\mathbf{k}_0$ and the positive z axis is ζ, so that only $\mathbf{E}_1^i$ represents the cylindrical vector waves that are incident on the interface $z=0$.

Following Eq. (2), the reflected beam and transmitted beam can be expanded in terms of the CVWFs, as follows:

$$\mathbf{E}^r = E_0 \sum_{m=-\infty}^{\infty} \int_0^{\frac{\pi}{2}} [a_m(\zeta)\mathbf{m}_{m\lambda}^{(1)}(-h) + b_m(\zeta)\mathbf{n}_{m\lambda}^{(1)}(-h)]\exp(-ihz)d\zeta \tag{6}$$

$$\mathbf{E}^t = E_0 \sum_{m=-\infty}^{\infty} \int_0^{\frac{\pi}{2}} [e_m(\zeta)\mathbf{m}_{m\lambda}^{(1)}(h) + f_m(\zeta)\mathbf{n}_{m\lambda}^{(1)}(h)]\exp(ihz)d\zeta \tag{7}$$

For the sake of brevity, only the expansions of the electric fields are written, and the corresponding expansions of the magnetic fields can be obtained with the following relations

$$\mathbf{H} = \frac{1}{i\omega\mu_0}\nabla\times\mathbf{E}, \quad \left[\mathbf{m}_{m\lambda}e^{ihz} \quad \mathbf{n}_{m\lambda}e^{ihz}\right] = \frac{1}{k_0}\nabla\times\left[\mathbf{n}_{m\lambda}e^{ihz} \quad \mathbf{m}_{m\lambda}e^{ihz}\right] \tag{8}$$

2.2 Description of electromagnetic fields within a chiral slab

The constitutive relations for a chiral medium can be expressed by [8, 9]

$$\mathbf{D} = \varepsilon_0\varepsilon_r\mathbf{E} + i\kappa\sqrt{\mu_0\varepsilon_0}\mathbf{H} \tag{9}$$

$$\mathbf{B} = \mu_0\mu_r\mathbf{H} - i\kappa\sqrt{\mu_0\varepsilon_0}\mathbf{E} \tag{10}$$

where κ is the chirality parameter.

The EM fields in a chiral medium ($\mathbf{E},\mathbf{H}$) are the sum of the right-handed waves ($\mathbf{E}_+,\mathbf{H}_+$) and left-handed waves ($\mathbf{E}_-,\mathbf{H}_-$). As discussed in [17], the CVWFs can be combined to represent ($\mathbf{E}_+,\mathbf{H}_+$) and ($\mathbf{E}_-,\mathbf{H}_-$). Then, the EM waves within the chiral slab (internal beam) that propagate towards the interface $z=d$ can be described by the following equations,

$$\begin{aligned}\mathbf{E}_1^w = E_0 \sum_{m=-\infty}^{\infty} \int_0^{\frac{\pi}{2}} &\Big\{c_m(\zeta)\left[\mathbf{m}_{m\lambda}^{(1)}(h_+) + \mathbf{n}_{m\lambda}^{(1)}(h_+)\right]\exp(ih_+z) \\ &+ d_m(\zeta)\left[\mathbf{m}_{m\lambda}^{(1)}(h_-) - \mathbf{n}_{m\lambda}^{(1)}(h_-)\right]\exp(ih_-z)\Big\}d\zeta\end{aligned} \tag{11}$$

$$\mathbf{H}_1^w = -i\frac{E_0}{\eta}\sum_{m=-\infty}^{\infty}\int_0^{\frac{\pi}{2}}\left\{c_m(\zeta)\left[\mathbf{m}_{m\lambda}^{(1)}(h_+)+\mathbf{n}_{m\lambda}^{(1)}(h_+)\right]\exp(ih_+z)\right.$$
$$\left. -d_m(\zeta)\left[\mathbf{m}_{m\lambda}^{(1)}(h_-)-\mathbf{n}_{m\lambda}^{(1)}(h_-)\right]\exp(ih_-z)\right\}d\zeta \tag{12}$$

and similarly, the EM waves towards the interface $z=0$ are governed by

$$\mathbf{E}_2^w = E_0\sum_{m=-\infty}^{\infty}\int_0^{\frac{\pi}{2}}\left\{c'_m(\zeta)\left[\mathbf{m}_{m\lambda}^{(1)}(-h_+)+\mathbf{n}_{m\lambda}^{(1)}(-h_+)\right]\exp(-ih_+z)\right.$$
$$\left. +d'_m(\zeta)\left[\mathbf{m}_{m\lambda}^{(1)}(-h_-)-\mathbf{n}_{m\lambda}^{(1)}(-h_-)\right]\exp(-ih_-z)\right\}d\zeta \tag{13}$$

$$\mathbf{H}_2^w = -i\frac{E_0}{\eta}\sum_{m=-\infty}^{\infty}\int_0^{\frac{\pi}{2}}\left\{c'_m(\zeta)\left[\mathbf{m}_{m\lambda}^{(1)}(-h_+)+\mathbf{n}_{m\lambda}^{(1)}(-h_+)\right]\exp(-ih_+z)\right.$$
$$\left. -d'_m(\zeta)\left[\mathbf{m}_{m\lambda}^{(1)}(-h_-)-\mathbf{n}_{m\lambda}^{(1)}(-h_-)\right]\exp(-ih_-z)\right\}d\zeta \tag{14}$$

where

$$h_\pm = \sqrt{k_\pm^2-\lambda^2}\ ,\quad k_\pm = k_0(\sqrt{\mu_r\varepsilon_r}\pm\kappa)\,,\quad \sqrt{\frac{\mu_0}{\varepsilon_0}}\sqrt{\frac{\mu_r}{\varepsilon_r}} = \eta_0\sqrt{\frac{\mu_r}{\varepsilon_r}} = \eta \tag{15}$$

2.3 Reflection and transmission of Gaussian beam by a chiral slab

The unknown expansion coefficients $a_m(\zeta)$, $b_m(\zeta)$ in Eq. (6), $e_m(\zeta)$, $f_m(\zeta)$ in Eq. (7), $c_m(\zeta)$, $d_m(\zeta)$ in Eqs. (11) and (12) as well as $c'_m(\zeta)$, $d'_m(\zeta)$ in Eqs. (13) and (14) can be determined by using the following boundary conditions

$$\left.\begin{array}{ll} E_{1r}^i + E_r^r = E_{1r}^w + E_{2r}^w & E_{1\phi}^i + E_\phi^r = E_{1\phi}^w + E_{2\phi}^w \\ H_{1r}^i + H_r^r = H_{1r}^w + H_{2r}^w & H_{1\phi}^i + H_\phi^r = H_{1\phi}^w + H_{2\phi}^w \end{array}\right\} \quad at \quad z=0 \tag{16}$$

$$\left.\begin{array}{ll} E_{1r}^w + E_{2r}^w = E_r^t & E_{1\phi}^w + E_{2\phi}^w = E_\phi^t \\ H_{1r}^w + H_{2r}^w = H_r^t & H_{1\phi}^w + H_{2\phi}^w = H_\phi^t \end{array}\right\} \quad at \quad z=d \tag{17}$$

where the subscripts r and ϕ respectively denote the r and ϕ components of the EM fields.

Eqs. (16) and (17) are valid for every value of $m=-M$, $-M+1$, …, M and $\zeta=0$ to $\pi/2$, where M is the convergence number of the summation of series, and then from the fields expansions the boundary conditions in Eq. (16) can be written as

$$I_{m,TE}(h)+a_m(\zeta) = c_m(\zeta)+d_m(\zeta)+c'_m(\zeta)+d'_m(\zeta) \tag{18}$$

$$I_{m,TM}(h)\cos\zeta - b_m(\zeta)\cos\zeta = c_m(\zeta)\frac{h_+}{k_+} - d_m(\zeta)\frac{h_-}{k_-} - c'_m(\zeta)\frac{h_+}{k_+} + d'_m(\zeta)\frac{h_-}{k_-} \tag{19}$$

$$I_{m,TE}(h)\cos\zeta - a_m(\zeta)\cos\zeta = \frac{\eta_0}{\eta}c_m(\zeta)\frac{h_+}{k_+} + \frac{\eta_0}{\eta}d_m(\zeta)\frac{h_-}{k_-} - \frac{\eta_0}{\eta}c'_m(\zeta)\frac{h_+}{k_+} - \frac{\eta_0}{\eta}d'_m(\zeta)\frac{h_-}{k_-} \tag{20}$$

$$I_{m,TM}(h)+b_m(\zeta) = \frac{\eta_0}{\eta}c_m(\zeta) - \frac{\eta_0}{\eta}d_m(\zeta) + \frac{\eta_0}{\eta}c'_m(\zeta) - \frac{\eta_0}{\eta}d'_m(\zeta) \tag{21}$$

and the boundary conditions in Eq. (17) as

$$c_m(\zeta)e^{ih_+d} + d_m(\zeta)e^{ih_-d} + c'_m(\zeta)e^{-ih_+d} + d'_m(\zeta)e^{-ih_-d} = e_m(\zeta)e^{ihd} \tag{22}$$

$$c_m(\zeta)\frac{h_+}{k_+}e^{ih_+d} - d_m(\zeta)\frac{h_-}{k_-}e^{ih_-d} - c'_m(\zeta)\frac{h_+}{k_+}e^{-ih_+d} + d'_m(\zeta)\frac{h_-}{k_-}e^{-ih_-d} = f_m(\zeta)\frac{h}{k_0}e^{ihd} \tag{23}$$

$$c_m(\zeta)e^{ih_+d} - d_m(\zeta)e^{ih_-d} + c'_m(\zeta)e^{-ih_+d} - d'_m(\zeta)e^{-ih_-d} = \frac{\eta}{\eta_0}f_m(\zeta)e^{ihd} \tag{24}$$

$$c_m(\zeta)\frac{h_+}{k_+}e^{ih_+d} + d_m(\zeta)\frac{h_-}{k_-}e^{ih_-d} - c'_m(\zeta)\frac{h_+}{k_+}e^{-ih_+d} - d'_m(\zeta)\frac{h_-}{k_-}e^{-ih_-d} = \frac{\eta}{\eta_0}e_m(\zeta)\frac{h}{k_0}e^{ihd} \tag{25}$$

From the system consisting of Eqs. (18)–(25), the unknown expansion coefficients can be determined. By substituting them into Eqs. (6), (7) and (11)-(14), the reflected, transmitted and internal beams can be obtained respectively.

3. NUMERICAL RESULTS AND DISCUSSIONS

In this paper, the focus will be on the normalized field intensity distributions, which are defined respectively by the following set of equations,

$$\left|(\mathbf{E}^i + \mathbf{E}^r)/E_0\right|^2 = (\left|E_r^i + E_r^r\right|^2 + \left|E_\phi^i + E_\phi^r\right|^2 + \left|E_z^i + E_z^r\right|^2)\Big/\left|E_0\right|^2 \tag{26}$$

$$\left|(\mathbf{E}_1^w + \mathbf{E}_2^w)/E_0\right|^2 = (\left|E_{1r}^w + E_{2r}^w\right|^2 + \left|E_{1\phi}^w + E_{2\phi}^w\right|^2 + \left|E_{1z}^w + E_{2z}^w\right|^2)\Big/\left|E_0\right|^2 \tag{27}$$

and

$$\left|\mathbf{E}^t/E_0\right|^2 = (\left|E_r^t\right|^2 + \left|E_\phi^t\right|^2 + \left|E_z^t\right|^2)\Big/\left|E_0\right|^2 \tag{28}$$

By substituting the r, ϕ and z components of the CVWFs into Eqs. (1), (6), (7), (11) and (13) [12], the r, ϕ and z components of the electric fields of the incident Gaussian beam, reflected beam, transmitted beam as well as internal beam can be obtained, and then the explicit expressions of Eqs. (26)-(28) can be derived.

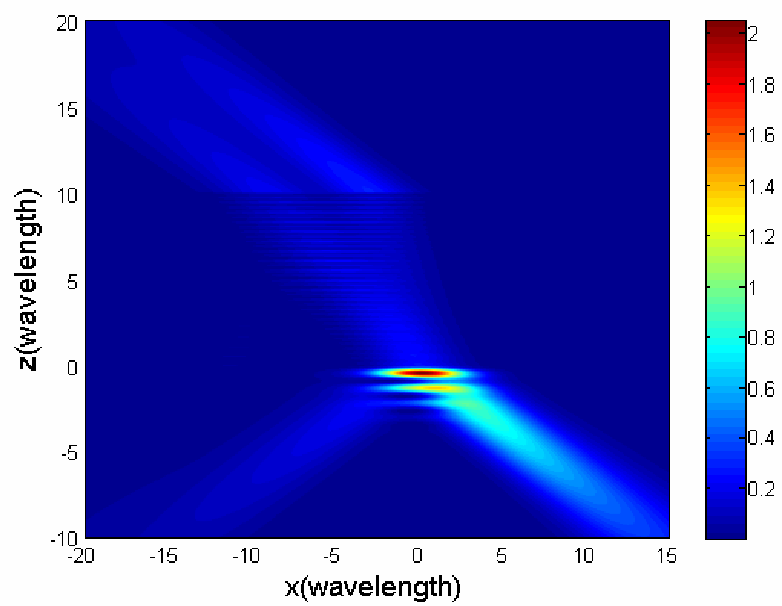

Fig.2. $\left|(\mathbf{E}^i + \mathbf{E}^r)/E_0\right|^2$, $\left|(\mathbf{E}_1^w + \mathbf{E}_2^w)/E_0\right|^2$ and $\left|\mathbf{E}^t/E_0\right|^2$ for a chiral slab illuminated by a TE polarized Gaussian beam

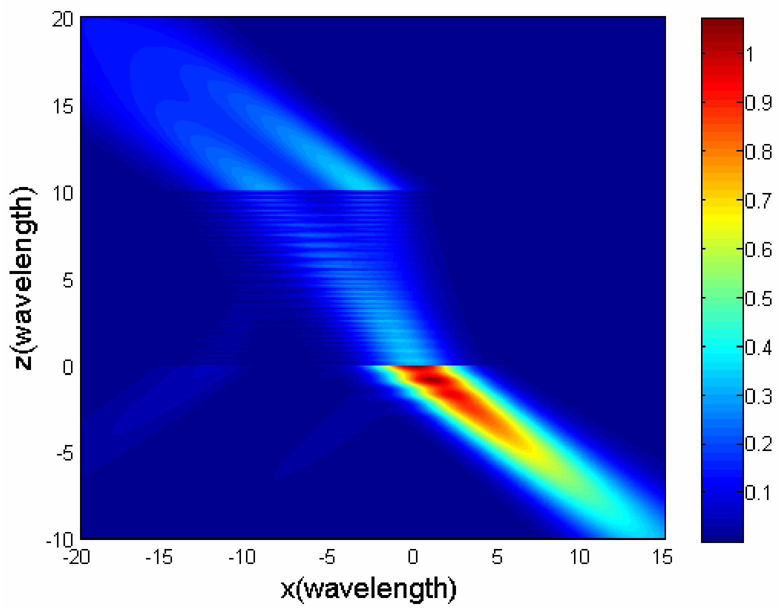

Fig.3. $\left|(\mathbf{E}^i+\mathbf{E}^r)/E_0\right|^2$, $\left|(\mathbf{E}_1^w+\mathbf{E}_2^w)/E_0\right|^2$ and $\left|\mathbf{E}^t/E_0\right|^2$ for the same model as in Fig.2 illuminated by a TM polarized Gaussian beam

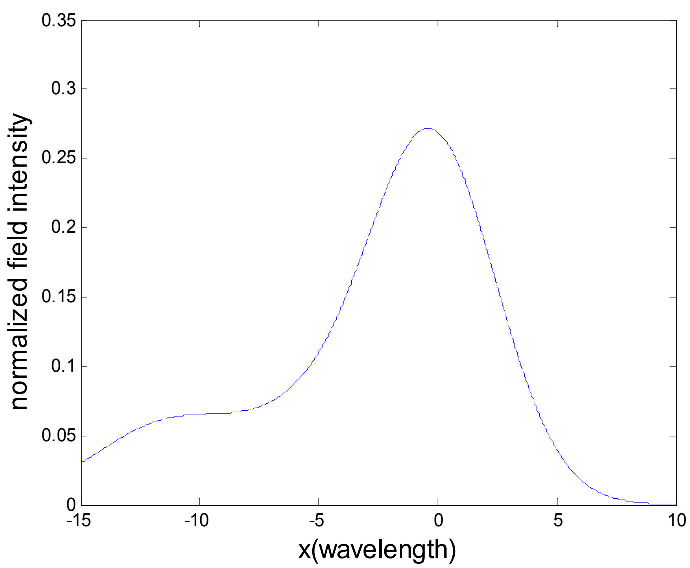

Fig.4. $\left|\mathbf{E}^r/E_0\right|^2$ for the same model as in Fig.2 at $z=0$ in the xOz plane illuminated by a TE polarized Gaussian beam

In the following calculations, the normalized field intensity distributions are shown in the xOz plane for a chiral slab ($\varepsilon_r=4$, $\mu_r=1$, $\kappa=0.8$) illuminated by a Gaussian beam (TE or TM polarized) with an angle of incidence $\beta=\arctan\sqrt{2}$ and $z_0=0$. The slab thickness is assumed to be $d=10\lambda_0$, with λ_0 as the wavelength of the incident Gaussian beam.

As for the problem in this paper of the Gaussian beam propagation through an infinite chiral slab, in numerical results the convergence number M is dependent on the beam waist radius w_0. To our computation, a better convergence accuracy (three or more digits of accuracy) of the fields series expansions can be readily achieved when $M \geq 20$ for the localized Gaussian beam model.

Figure 2 shows the normalized field intensity distributions for a chiral slab illuminated by a TE polarized Gaussian beam with $w_0 = 2\lambda_0$. From Fig.2 we can see that inside the chiral slab an incident Gaussian beam splits into two waves, corresponding to the RCP and LCP waves respectively. Due to the refraction of the RCP and LCP waves at the interface $z = d$, two distinct transmitted waves appear in the region $z > d$, which is also observed in Fig.3. The normalized field intensity distributions are displayed in Fig.3 for the same model as in Fig.2 but illuminated by a TM polarized Gaussian beam with $w_0 = 2\lambda_0$. In Fig.3, the normalized field intensity of the reflected beam becomes too much smaller, as a result of the Brewster angle phenomenon.

The normalized reflected field intensity distribution $\left|\mathbf{E}^r / E_0\right|^2 = \left(\left|E_r^r\right|^2 + \left|E_\phi^r\right|^2 + \left|E_z^r\right|^2\right) \Big/ \left|E_0\right|^2$ versus x is plotted in Fig.4 for the same model as in Fig.2 at $z = 0$ in the xOz plane, for incidence of a TE polarized Gaussian beam with $w_0 = 3\lambda_0$. In Fig.4, different from the assumption that the beam waist center of the incident Gaussian beam is located at $x = 0$, the first field intensity peak in the reflected beam is shifted along the negative x axis by a distance of about $0.41\lambda_0$, which is known as the lateral shift associated with an incident shaped beam [8].

In experiment, it is more attractive to realize the scenario of this paper in the millimeter-wave regime. In [18], Jaggard et al. presented a macroscopic model of the interaction of EM waves with chiral structures, i.e. electrically small perfect conductor helices, right- or left-handed. Then, a chiral slab can be fabricated by embedding many short metallic right- or left-handed helices of arbitrary orientation in a dielectric slab. A dielectric hybrid-mode horn antenna has been devised and analyzed theoretically [19], which can be used to radiate up to 98% of the power into the fundamental Gaussian mode [20]. So, it will be a realistic experimental design to illuminate a collection of randomly oriented short metallic helices of the same handedness by collimated Gaussian beams radiated from a dielectric hybrid-mode horn.

4. CONCLUSIONS

By the use of the field expansions in terms of the CVWFs, an approach to compute the reflection and transmission of an incident Gaussian beam by a chiral slab is presented. Since there are two refractive indices corresponding to the RCP and LCP waves within the chiral slab, two distinct transmitted waves are observed in the transmitted beam. A lateral shift in the reflected beam is also demonstrated. As a result, this study provides an exact analytical model for interpretation of Gaussian beam propagation phenomena through a chiral slab, and the method can also be extended to other cases such as uniaxial chiral, biaxial and gyrotropic anisotropic slabs. We hope that this study may lend support to research on the EM properties of chiral media.

REFERENCES

1. C. F. Bohren, "Light scattering by an optically active sphere" Chemical Physics Letters **29**, 458-462 (1974).
2. C. F. Bohren, "Scattering of electromagnetic waves by an optically active cylinder," Journal of Colloid and Interface Science **66**, 105-109 (1978).
3. M. P. Silverman," Reflection and refraction at the surface of a chiral medium: comparison of gyrotropic constitutive relations invariant or noninvariant under a duality transformation," J. Opt. Soc. Am. A **3**, 830-837 (1986).
4. S. Bassiri, C. H. Papas, and N. Engheta, "Electromagnetic wave propagation through a

dielectric-chiral interface and through a chiral slab," J. Opt. Soc. Am. A **5**, 1450-1459 (1988).
5. M. Yokota, S. L. He, and T. Takenaka, "Scattering of a Hermite-Gaussian beam field by a chiral sphere," J. Opt. Soc. Am. A **18**, 1681-1689 (2001).
6. A. Lakhtakia, V. K. Varadan, and V. V. Varadan, "Excitation of a planar achiral/chiral interface by near fields," Journal of Wave-Material Interaction **3**, 231-241 (1988).
7. D. J. Hoppe and Y. Rahmat-Samii, "Gaussian beam reflection at a dielectric-chiral interface," Journal of Electromagnetic Waves and Applications **6**, 603-624 (1992).
8. Y. Y. Huang, W. T. Dong, L. Gao, and C. W. Qiu, "Large positive and negative lateral shifts near pseudo-Brewster dip on reflection from a chiral metamaterial slab," Optics Express **19**, 1310-1323 (2011).
9. Q. C. Shang, Z. S. Wu, T. Qu, Z. J. Li, Lu. B, and L. Gong, "Analysis of the radiation force and torque exerted on a chiral sphere by a Gaussian beam," Optics Express 21, 8677-8688 (2013).
10. H. Y. Zhang, Y. P. Han, and G. X. Han, "Expansion of the electromagnetic fields of a shaped beam in terms of cylindrical vector wave functions," J. Opt. Soc. Am. B **24**, 1383–1391 (2007).
11. V. V. Varadan, A. Lakhtakia, and V. K. Varadan, Field Representations and Introduction to Scattering, North Holland, 1991, Eq.(4.25) in Chap 4.
12. J.A. Stratton, Electromagnetic Theory, McGraw-Hill, New York, 1941, Chap.VII.
13. L. W. Davis, "Theory of electromagnetic beam," Phys. Rev. A **19**, 1177–1179 (1979).
14. G. Gouesbet, "Validity of the localized approximation for arbitrary shaped beam in the generalized Lorenz-Mie theory for spheres," J. Opt. Soc. Am. A **16**, 1641–1650 (1999).
15. G. Gouesbet, J. A. Lock, and G. Gréhan, "Generalized Lorenz–Mie theories and description of electromagnetic arbitrary shaped beams: Localized approximations and localized beam models, a review," JQSRT **112**, 1–27 (2011).
16. G. Gouesbet, G. Gréhan, and K. F. Ren, "Rigorous justification of the cylindrical localized approximation to speed up computations in the generalized Lorenz–Mie theory for cylinders," J. Opt. Soc. Am. A **15**, 511–523 (1998).
17. Y. M. Zhai, H. Y. Zhang and Y. F. Sun, "On-axis Gaussian beam scattering by a chiral cylinder," J. Opt. Soc. Am. A **29**, 2509–2513 (2012).
18. D. L. Jaggard, A. R. Mickelson and C. H. Papas, "On Electromagnetic Waves in Chiral Media," Applied Physics **18**, 211-216 (1979).
19. E. Lier, "A Dielectric Hybrid Mode Antenna Feed: A Simple Alternative to the Corrugated Horn," IEEE Trans Antennas Propag **34**, 21–29 (1986).
20. W. B. Dou and Z. L. Sun, "A dielectric hybrid-mode horn as a Gaussian beam-mode antenna in 3mm band" Microwave and Optical Technology Letters **6**, 475-478 (1993).